

Characterization of Hydrogen Bond Lengths in Watson–Crick Base Pairs by Cross-Correlated Relaxation

Roland Riek

Institut für Molekularbiologie und Biophysik, Eidgenössische Technische Hochschule Hönggerberg, CH-8093 Zürich, Switzerland

Received October 2, 2000; revised December 20, 2000

Hydrogen bond lengths in Watson–Crick base pairs can be characterized by cross-correlated relaxation between ^1H chemical shift anisotropy and dipole–dipole coupling of ^1H and its hydrogen bond acceptor ^{15}N . As a reference, the cross-correlated relaxation between ^1H chemical shift anisotropy and dipole–dipole coupling of ^1H and its hydrogen bond donor ^{15}N is used. With the two measured cross-correlated relaxation rates, an apparent hydrogen bond length can be determined, which is composed by the hydrogen bond length multiplied by a term representing the amplitude of interbase motions. Data are presented for the $^{15}\text{N}_3\text{--}^1\text{H}_3\text{--}^{15}\text{N}_1$ hydrogen bonds in A = T base pairs of the *Antennapedia* homeodomain–DNA complex with a correlation time of global rotational diffusion of 20 ns. © 2001 Academic Press

Key Words: NMR; cross-correlated relaxation; TROSY; hydrogen bonds; Watson–Crick base pair.

Hydrogen bonds are key elements in three-dimensional structures of proteins and nucleic acids as well as for intermolecular recognition. However, usually their presence in biological macromolecules can only indirectly be inferred from experimental data (1). The observation of scalar couplings across hydrogen bonds now provides direct evidence for these interactions, and these data have been reported for Watson–Crick base pairs in nucleic acids (2, 3) and for hydrogen bonds in proteins (4). Here, we show that by measuring cross-correlated relaxation (5–15) across the hydrogen bond between ^1H chemical shift anisotropy (CSA)¹ and dipole–dipole (DD) coupling of ^1H and its hydrogen bond acceptor ^{15}N , an apparent hydrogen bond length can be determined, which characterizes the length of the hydrogen bond in combination with its dynamical fluctuation.

The rate of cross-correlated relaxation between axial CSA of spin I and the DD-coupling between spin I and spin S in a large

spherical molecule with fast internal motions is given by

$$R_C = \frac{4P_2(\vartheta)}{15}(\gamma_I B_0 \Delta\sigma_I)(\hbar\gamma_I\gamma_S/r_{IS}^3)\tau_c S^2, \quad [1]$$

where r_{IS} is the internuclear distance, $\Delta\sigma_I$ is the CSA tensor of nucleus I, B_0 is the static magnetic field, γ_I and γ_S are the gyromagnetic ratios of I and S (5, 6, 14, 15), $P_2(\vartheta) = \frac{1}{2}(3(\cos(\vartheta))^2 - 1)$ is the second-order Legendre polynomial evaluated at the angle ϑ between the long principal axis of the CSA tensor and the internuclear vector, and S is the generalized order parameter (16).

The relaxation rates of interest in this publication are $^{\text{H}\cdot\text{N}}R_C$, the cross-correlated relaxation rate across the hydrogen bond between ^1H CSA and DD coupling of ^1H and its hydrogen bond acceptor ^{15}N , and $^{\text{H}\cdot\text{N}}R_C$, the cross-correlated relaxation rate within the imino group between ^1H CSA and DD coupling of ^1H and its covalently attached hydrogen bond donor ^{15}N (see Fig. 1a). The ratio between the two relaxation rates is

$$\frac{^{\text{H}\cdot\text{N}}R_C}{^{\text{H}\cdot\text{N}}R_C} = \frac{P_2(\vartheta) \cdot ^{\text{H}\cdot\text{N}}S^2 \cdot ^{\text{H}\cdot\text{N}}r^3}{P_2(\vartheta + \delta) \cdot ^{\text{H}\cdot\text{N}}S^2 \cdot ^{\text{H}\cdot\text{N}}r^3}, \quad [2]$$

where $^{\text{H}\cdot\text{N}}r$ and $^{\text{H}\cdot\text{N}}r$ are the two characteristic distances for a hydrogen bond (see Fig. 1a), and δ is the angle by which the hydrogen bond deviates from linearity. The order parameter $^{\text{H}\cdot\text{N}}S$ characterizes the amplitude of the intrabase motion of the covalent bond $^{15}\text{N}\text{--}^1\text{H}$, and $^{\text{H}\cdot\text{N}}S$ characterizes the amplitude of the interbase motion of the hydrogen bond $^1\text{H}\cdot^{15}\text{N}$ (Fig. 1a).

If a linear hydrogen bond is assumed the two relaxation rates differ only by the two distances $^{\text{H}\cdot\text{N}}r$ and $^{\text{H}\cdot\text{N}}r$ and the two order parameters $^{\text{H}\cdot\text{N}}S$ and $^{\text{H}\cdot\text{N}}S$. Thus, measuring the two cross-correlated relaxation rates $^{\text{H}\cdot\text{N}}R_C$ and $^{\text{H}\cdot\text{N}}R_C$ an apparent hydrogen bond length $^{\text{H}\cdot\text{N}}r_{\text{apparent}}$ can be determined:

$$\begin{aligned} ^{\text{H}\cdot\text{N}}r_{\text{apparent}} &= ^{\text{H}\cdot\text{N}}r \cdot \sqrt[3]{\frac{^{\text{H}\cdot\text{N}}S^2}{^{\text{H}\cdot\text{N}}S^2}} \\ &= ^{\text{H}\cdot\text{N}}r \cdot \sqrt[3]{\frac{^{\text{H}\cdot\text{N}}R_C}{^{\text{H}\cdot\text{N}}R_C}}. \end{aligned} \quad [3]$$

¹ Abbreviations used: CSA, chemical shift anisotropy; DD, dipole–dipole; $^{\text{H}\cdot\text{N}}R_C$, cross-correlated relaxation rate across the hydrogen bond between ^1H CSA and DD coupling of ^1H and its hydrogen bond acceptor ^{15}N ; $^{\text{H}\cdot\text{N}}R_C$, cross-correlated relaxation rate within the imino group between ^1H CSA and DD coupling of ^1H and its covalently attached hydrogen bond donor ^{15}N ; $^{\text{H}\cdot\text{N}}r_{\text{apparent}}$, the apparent hydrogen bond length; $^{\text{H}\cdot\text{N}}S$, order parameter of the hydrogen bond; $^{\text{H}\cdot\text{N}}S$, order parameter of the covalent bond $^{15}\text{N}\text{--}^1\text{H}$.

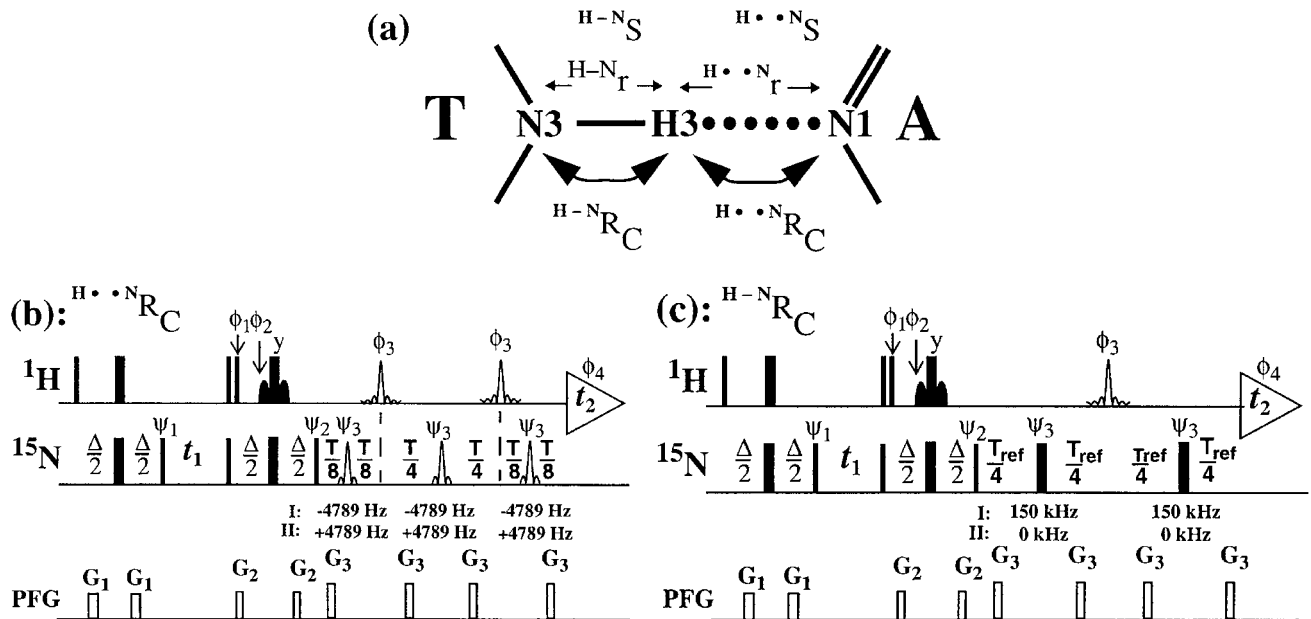


FIG. 1. (a) Cartoon of the hydrogen bond $^{15}N-^1H3 \cdot \cdot ^{15}N1$ in A=T base pairs with the corresponding relaxation rates and internuclear distances $H-N_r$ and $H \cdot \cdot N_r$. (b) and (c) [$^{15}N, ^1H$]-ZQ TROSY experiments for measurements of cross-correlated relaxation rate across the hydrogen bond $H \cdot \cdot N_{RC}$ between 1H3 CSA and $^1H3 \cdot \cdot ^{15}N1$ DD coupling in A=T base pairs and of cross-correlated relaxation rate $H-N_{RC}$ between 1H3 CSA and $^1H3-^{15}N3$ DD coupling, respectively. The actual cross-correlated relaxation rates rely on the ratio of the peak volumes of the two interleaved measured subexperiments I and II, which differs only in the offset of the ^{15}N softpulses as indicated in the scheme. The hydrogen bond distance $H \cdot \cdot N_r$ (see (a)) is calculated from the ratio of the two measured cross-correlated relaxation rates $H \cdot \cdot N_{RC}$ and $H-N_{RC}$ in (b) and (c) and from the covalent $^1H3-^{15}N3$ distance $H-N_r$ according to Eq. [5]. In the experimental schemes, narrow and wide bars indicate nonselective 90° and 180° pulses applied at the 1H and the ^{15}N frequencies, with the carrier offsets placed at 12.8 and 159.5 ppm, respectively, if not otherwise specified. Water is handled by the application of off-resonance water-selective 90° rf-pulses with length 1.5 ms indicated by shaded shapes on the line 1H (22). The delays are $\Delta = 5.4$ ms, $T = 130$ ms, and $T_{ref} = 24$ ms. The line marked PFG indicates the pulsed magnetic field gradients applied along the z-axis with a duration of 0.8 ms and an amplitude of G_1 : 10 G/cm, G_2 : 12 G/cm, and G_3 : 15 G/cm. The phases for the rf-pulses are $\Phi_1 = \{x\}$, $\Phi_2 = \{-x\}$, $\Phi_3 = \{x\}$, $\Phi_4 = \{x, -x, -y, y\}$, $\Psi_1 = \{y, -y, x, -x\}$, $\Psi_2 = \{y\}$; $\Psi_3 = \{x, x, x, x, -x, -x, -x, -x\}$; x on all pulses without phase specification. The 180° pulses with phase Φ_3 consist of a refocusing REBURP pulse (23), with a duration of 1 ms. In (b), the 180° pulses with phase Ψ_3 consist of a Gaussian profile with a duration of 450 μs and an offset of -4789 Hz for subexperiment I and $+4789$ Hz for subexperiment II, respectively. The 180° pulses with phase Ψ_3 in subexperiment II excite the hydrogen bond acceptor $^{15}N1$ resonances at 222.5 ppm to suppress the cross-correlated relaxation across the hydrogen bond. For subexperiment I the 180° pulses with phase Ψ_3 are not needed, but one used to minimize any artefacts, i.e., the partial excitation of the hydrogen bond donor N3 resonances in both subexperiments. In subexperiment II of (c), the 180° pulses with phase Ψ_3 were set on resonance to 159.5 ppm to suppress the cross-correlated relaxation $H-N_{RC}$ between 1H3 CSA and $^1H3-^{15}N3$ DD coupling during the delay T_{ref} . As in (b) for subexperiment I, no 180° pulses with phase Ψ_3 are needed, but set of resonance by -150 kHz to avoid any artefacts between the two subexperiments. For each individual data set recorded with I and II in (b) and (c), a complex interferogram is obtained by recording a second FID for each t_1 delay, with $\Phi_1 = \{-x\}$, $\Phi_2 = \{x\}$, $\Phi_4 = \{x, -x, y, -y\}$, and $\Psi_2 = \{-y\}$, which results in a phase-sensitive 2D [$^1H, ^{15}N$] correlation spectrum that contains only the slowly relaxing component of the 2D $^{15}N-^1H$ multiplet. The two subspectra I and II of (b) and (c) were measured interleaved and stored separately. For the data processing the procedure of Kay *et al.* (24) was used. The given length of the soft pulses is optimized for a magnetic field of 750 MHz 1H -frequency.

Since the order parameter S characterizes the amplitude in motion, the ratio of the two order parameters describes the motional amplitude of the hydrogen bond relative to the motional amplitude of the donor base. Thus, the apparent hydrogen bond length is a product of a geometric factor and a motional factor. For a rigid Watson-Crick base pair $H \cdot \cdot N_{r,apparent} = H \cdot \cdot N_r$. For a Watson-Crick base pair with interbase motions $H \cdot \cdot N_{r,apparent} > H \cdot \cdot N_r$.

The hydrogen bonds in Watson-Crick base pairs might deviate from linearity. In the crystal structure of the *Antennapedia* homeodomain-DNA complex (18) the deviation from linearity is smaller than 10° ($\delta < 10^\circ$). The contribution of such small deviations to the determination of an apparent hydrogen bond

length is less than 10%, and therefore within the precision of the determination of the hydrogen bond length (see also caption to Fig. 3a).

In the following we focus on hydrogen bond lengths determination of A=T base pairs. The experimental pulse scheme for measuring the cross-correlated relaxation rate across the hydrogen bond $H \cdot \cdot N_{RC}$ is composed of two subexperiments termed I and II (Fig. 1b). It is based on a [$^{15}N, ^1H$]-ZQ-TROSY experiment as described previously (17) extended by a delay T . The 180° 1H -pulses during T refocus the chemical shifts and any scalar couplings (for example $^1J_{HN}$, $^hJ_{HN}$). In subexperiment I, cross-correlated relaxation across the hydrogen bond is active during the time period T , since the 180° pulses with phase Ψ_3 are

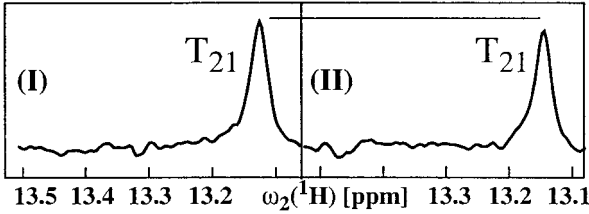


FIG. 2. Cross sections of subexperiment I and subexperiment II of the pulse sequence Fig. 1b through the cross-peak of the $^{15}\text{N}_3, ^1\text{H}_3$ moiety of T21 of the *Antennapedia* homeodomain- $^{13}\text{C}, ^{15}\text{N}$ -labeled DNA complex (Fig. 3c) recorded on a Bruker DRX 750 spectrometer using a triple-resonance probehead equipped with a z-gradient coil. In subexperiment II, cross-correlated relaxation across the hydrogen bond is suppressed, which results in lower intensity of the cross peak compared to the corresponding control experiment I. The NMR experiments in Figs. 1b and 1c were recorded at a concentration of 0.8 mM at 4°C . The measuring time for Fig. 1b was 70 h, for Fig. 1c 6 h. The acquired data size was in both experiments 50×1024 complex points, with $t_{1\text{max}} = 12$ ms and $t_{2\text{max}} = 170$ ms. The assignments were taken from Ref. (25).

set off-resonance (see Fig. 1b). Thus, the peak volume $^{\text{H}\cdot\text{N}}A_{\text{I}} \propto \frac{1}{2}(\text{Exp}[-T[R_2 + ^{\text{H}\cdot\text{N}}R_{\text{C}}]] + \text{Exp}[-T[R_2 - ^{\text{H}\cdot\text{N}}R_{\text{C}}]])$. R_2 is the non-cross-correlated part of the transverse relaxation of the involved hydrogen H3.

In subexperiment II, the 180° pulses with phase Ψ_3 are on resonance on the hydrogen bond acceptor N1 (222.5 ppm) and, therefore, suppress the cross-correlated relaxation rate across the hydrogen bond (otherwise the two subexperiments I and II are identical). The corresponding peak volume of subexperiment II $^{\text{H}\cdot\text{N}}A_{\text{II}} \propto \text{Exp}[-T R_2]$. Figure 2 shows cross sections through the cross-peak of the $^{15}\text{N}_3, ^1\text{H}_3$ -moiety of T21 of the *Antennapedia* homeodomain $^{15}\text{N}, ^{13}\text{C}$ -labeled DNA complex. The lower intensity of the cross peak of subexperiment II compared to the corresponding control experiment I is due to the suppression of the cross-correlated relaxation across the hydrogen bond.

From the ratio of peak volumes of subexperiment I, $^{\text{H}\cdot\text{N}}A_{\text{I}}$, and of subexperiment II, $^{\text{H}\cdot\text{N}}A_{\text{II}}$, $^{\text{H}\cdot\text{N}}R_{\text{C}}$, is calculated as

$$^{\text{H}\cdot\text{N}}R_{\text{C}} = \frac{1}{T} \text{acosh} \left(\frac{^{\text{H}\cdot\text{N}}A_{\text{I}}}{^{\text{H}\cdot\text{N}}A_{\text{II}}} \right). \quad [4]$$

Similarly, using the pulse sequence of Fig. 1c, the cross-correlated relaxation rate $^{\text{H}\cdot\text{N}}R_{\text{C}}$ between $^1\text{H}_3$ CSA and $^1\text{H}_3$ - $^{15}\text{N}_3$ DD coupling is measured. Finally, in accordance with Eq. [3] the apparent hydrogen bond length $^{\text{H}\cdot\text{N}}r_{\text{apparent}}$ is obtained from

$$^{\text{H}\cdot\text{N}}r_{\text{apparent}} = ^{\text{H}\cdot\text{N}}r \sqrt[3]{\frac{T \cdot \text{acosh} \left(\frac{^{\text{H}\cdot\text{N}}A_{\text{I}}}{^{\text{H}\cdot\text{N}}A_{\text{II}}} \right)}{T_{\text{ref}} \cdot \text{acosh} \left(\frac{^{\text{H}\cdot\text{N}}A_{\text{I}}}{^{\text{H}\cdot\text{N}}A_{\text{II}}} \right)}}. \quad [5]$$

As can be inferred from Eq. [5], the apparent hydrogen bond length $^{\text{H}\cdot\text{N}}r_{\text{apparent}}$ depends strongly on the ratio $^{\text{H}\cdot\text{N}}A_{\text{I}}/^{\text{H}\cdot\text{N}}A_{\text{II}}$ of experiment Fig. 1b, as shown in Fig. 3a. Thus, hydrogen

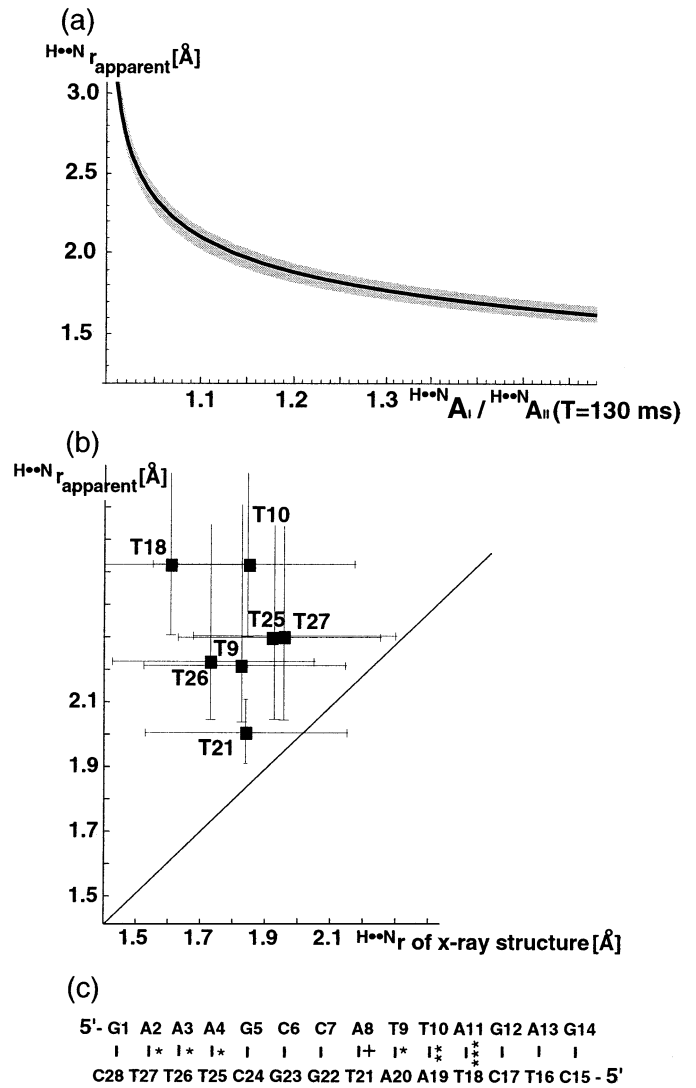


FIG. 3. (a) Hydrogen bond length $^{\text{H}\cdot\text{N}}r_{\text{apparent}}$ vs the ratio of the peak volumes $^{\text{H}\cdot\text{N}}A_{\text{I}}/^{\text{H}\cdot\text{N}}A_{\text{II}}$ of experiment of Fig. 1b according to Eq. [5]. The black curve was plotted with a N-H bond distance $^{\text{H}\cdot\text{N}}r = 0.98 \text{ \AA}$, $\vartheta = 20^\circ$, and the angle δ between the covalent and the hydrogen bond vectors of the distances $^{\text{H}\cdot\text{N}}r$ and $^{\text{H}\cdot\text{N}}r$ is 5° . The grey region was plotted covering the following parameters: $0.98 < ^{\text{H}\cdot\text{N}}r < 1.02 \text{ \AA}$, $0^\circ < \vartheta < 20^\circ$, and $0^\circ < \delta < 10^\circ$. The ratio $^{\text{H}\cdot\text{N}}A_{\text{I}}/^{\text{H}\cdot\text{N}}A_{\text{II}} = 1.5$ measured in experiment of Fig. 1c was used. (b) Hydrogen bond distance $^{\text{H}\cdot\text{N}}r_{\text{apparent}}$ obtained by cross-correlated relaxation vs hydrogen bond distance extracted from the X-ray structure of the *Antennapedia* homeodomain-DNA complex (18). The hydrogen bond distances obtained by cross-correlated relaxation were measured with a *Antennapedia* homeodomain-DNA complex with the fully $^{13}\text{C}, ^{15}\text{N}$ -labeled DNA duplex (see Fig. 2). Each experiment was measured three times and the average volume ratios of the three experiments were used. Hydrogen bond distances from the two X-ray structures with a resolution of 2.4 \AA (18; PDB accession code: 9ANT) were obtained assuming $^{\text{H}\cdot\text{N}}r = 0.98 \text{ \AA}$. The average hydrogen bond lengths are plotted with corresponding error bars, which are estimated based on the two available X-ray structures and on the resolution of the diffraction data according to Brünger (26). (c) DNA sequence of the *Antennapedia* homeodomain-DNA complex. The fitted average parameters $^{\text{H}\cdot\text{N}}S/^{\text{H}\cdot\text{N}}S$ for each measured hydrogen bond are indicated by + for $1 < ^{\text{H}\cdot\text{N}}S/^{\text{H}\cdot\text{N}}S < 1.2$, * for $1.2 < ^{\text{H}\cdot\text{N}}S/^{\text{H}\cdot\text{N}}S < 1.4$, ** for $1.4 < ^{\text{H}\cdot\text{N}}S/^{\text{H}\cdot\text{N}}S < 1.7$, and *** for $^{\text{H}\cdot\text{N}}S/^{\text{H}\cdot\text{N}}S > 1.7$, respectively.

bond lengths can be measured in principle accurately, even if variation in length of the covalent binding $^{\text{H}\cdot\text{N}}r$ and nonperfect linearity of the hydrogen bond are taken into consideration (for details see caption to Fig. 3). The major limitation of the approach presented here is that only a lower limit for $^{\text{H}\cdot\text{N}}r_{\text{apparent}}$ can be obtained for hydrogen bonds between two bases with large interbase motions. The measured volume ratios $^{\text{H}\cdot\text{N}}A_{\text{I}}/^{\text{H}\cdot\text{N}}A_{\text{II}}$ for apparent hydrogen bonds lengths longer than 2.3 Å are between 1.05 and 1.0 (see Fig. 3a). These values are not distinguishable in the experimental data set due to the signal to noise.

For the *Antennapedia* homeodomain ^{15}N , ^{13}C -labeled DNA complex (Fig. 3c) with a correlation time of global rotational diffusion of 20 ns (7), apparent hydrogen bond lengths $^{15}\text{N}3\text{--}^1\text{H}3\cdot\cdot^{15}\text{N}1$ in A = T base pairs were obtained (Fig. 3b). For the central Watson–Crick base pair A8 = T21 (Fig. 3c) the apparent hydrogen bond seems to be shorter than for the other A = T base pairs. The measured apparent hydrogen bond length of A8 = T21 is 1.9 Å. For all the other hydrogen bonds only a lower limit of 2 Å or 2.3 Å can be obtained, as shown in Fig. 3b. Since the apparent hydrogen bond length is a combination of dynamic and length of the hydrogen bond it describes its quality. Thus, the hydrogen bond of A8 = T21 is in respect to motion and length the strongest hydrogen bond measured.

In a comparison with the hydrogen bond lengths extracted from the crystal structures (18) the apparent hydrogen bond length $^{15}\text{N}3\text{--}^1\text{H}3\cdot\cdot^{15}\text{N}1$ for the central base pair A8 = T21 is similar in length. The close agreement between the apparent hydrogen bond length and the hydrogen bond length extrapolated from the crystal structure implies that the central base pair A8 = T21 seems to be quite rigid. In contrast, the apparent hydrogen bond lengths of the other base pairs are longer than the corresponding hydrogen bond length of the crystal structure (Fig. 3b). These observations are explained by interbase motions (see above). By fitting the apparent hydrogen bond length $^{\text{H}\cdot\text{N}}r_{\text{apparent}}$ with $^{\text{H}\cdot\text{N}}r$ the motional factor $^{\text{H}\cdot\text{N}}S/^{\text{H}\cdot\text{N}}S$ is obtained (Fig. 3c). As can be inferred from Fig. 3c the amplitude of the motion of the hydrogen bond relative to the donor base seems to increase towards the termini. Terminal fraying and concomitant larger motions are usually observed in small DNA duplexes, although not to such an extent as now demonstrated for the hydrogen bonds. Further, one large difference is observed for the hydrogen bond $^{15}\text{N}3\text{--}^1\text{H}3\cdot\cdot^{15}\text{N}1$ of the base pair T18 = A11 (Fig. 3b). In the crystal structures the hydrogen bond length is between 1.4 and 1.8 Å; the NMR measurements yield a lower limit of 2.3 Å. To fit the two hydrogen bond values a ratio $^{\text{H}\cdot\text{N}}S/^{\text{H}\cdot\text{N}}S > 1.7$ is calculated, which implies motions with large amplitudes between the bases of the Watson–Crick base pair. The interbase motion is therefore larger by at least a factor 1.7 than the intrabase motion. The finding that some interbase motions might occur between T18 = A11 is supported by the observed different conformations in the crystallographically independent complexes of the N-terminal arm of the homeodomain, which fits into the major groove with close contacts to

the base of T18 (in the X-ray structure Arg 5 makes a hydrogen bond to the O2 of T18).

Experiments similar to those in Figs. 1b and 1c were performed to determine the apparent hydrogen bond length $\text{N}\text{--}\text{H}\cdot\cdot\text{N}$ in $\text{G}\equiv\text{C}$ base pairs. However, due to the longer hydrogen bond length when compared to the corresponding hydrogen bond length in A = T base pairs (19) only a lower limit of 2 Å could be achieved (data not shown).

Finally, we would like to mention that the detection of tautomers in which hydrogen atoms become attached to the donor atom of the hydrogen bond could be easily detected via cross-correlated relaxation, since cross-correlated relaxation depends on the third power of the distance r_{IS} (see Eq. [1]). A population of 5% or more would be observed. In the *Antennapedia* homeodomain–DNA complex no tautomers for A = T base pairs were found.

In conclusion, we have shown that with cross-correlated relaxation apparent hydrogen bond distances which describe the dynamics and the length of a hydrogen bond can be obtained. This approach is an attractive additional tool to hydrogen bond observation based on scalar couplings (2, 3, 19), chemical shifts (19, 20), and hydrogen/deuterium exchange measurements (21) in DNA and RNA molecules.

ACKNOWLEDGMENTS

We thank Prof. Dr. Kurt Wüthrich and Prof. Dr. Masatsune Kainosho for making the *Antennapedia* homeodomain–DNA complex and NMR equipment available. We thank Dr. Peter Luginbühl for careful reading and helpful discussions.

REFERENCES

1. G. A. Jeffrey and W. Saenger, "Hydrogen Bonding in Biological Structures," Springer-Verlag, Berlin (1991).
2. A. J. Dingley and S. Grzesiek, Direct observation of hydrogen bonds in nucleic acid base pairs by internucleotide $^2J_{\text{NN}}$ couplings, *J. Am. Chem. Soc.* **120**, 8293–8297 (1998).
3. K. Pervushin, A. Ono, C. Fernández, T. Syzperski, M. Kainosho, and K. Wüthrich, NMR scalar couplings across Watson–Crick base pair hydrogen bonds in DNA observed by transverse relaxation optimized spectroscopy, *Proc. Natl. Acad. Sci. USA* **95**, 14,147–14,151 (1998).
4. F. Cordier and S. Grzesiek, Direct observation of hydrogen bonds in proteins by interresidue $^3J_{\text{NC}'}$ scalar couplings, *J. Am. Chem. Soc.* **121**, 1601–1602 (1999).
5. M. Goldman, Interference effects in the relaxation of a pair of unlike spin-1/2, *J. Magn. Reson.* **60**, 437–452 (1984).
6. R. Brüschweiler and R. R. Ernst, Molecular-dynamics monitored by cross-correlated cross relaxation of spins quantized along orthogonal axes, *J. Chem. Phys.* **96**, 1758–1766 (1991).
7. S. Wimperis and G. Bodenhausen, Relaxation-allowed cross-peaks in two-dimensional NMR correlation spectroscopy, *Mol. Phys.* **66**, 897–919 (1989).
8. B. Reif, M. Hennig, and C. Griesinger, Direct measurement of angles between bond vectors in high-resolution NMR, *Science* **276**, 1230–1233 (1997).

9. D. W. Yang, R. Konrat, L. E. Kay, A multidimensional NMR experiment for measurement of the protein dihedral angle ψ based on cross-correlated relaxation between ($H\alpha$ - $^{13}C\alpha$)-H-1 dipolar and C-13' chemical shift anisotropy mechanisms, *J. Am. Chem. Soc.* **119**, 11,938–11,940 (1997).
10. X. Feng, Y. K. Lee, D. Sandstrom, M. Eden, H. Maisel, A. Sebald, and M. H. Levitt, Direct determination of a molecular torsional angle by solid-state NMR, *Chem. Phys. Lett.* **257**, 314–320 (1996).
11. B. Brutscher, N. R. Skrynnikov, T. Bremi, R. Bruschweiler, and R. R. Ernst, Quantitative investigation of dipole-CSA cross-correlated relaxation by ZQ/DQ spectroscopy, *J. Magn. Reson.* **130**, 346–351 (1998).
12. E. Chiarparin, P. Pelupessy, R. Ghose, and G. Bodenhausen, Relaxation of two-spin coherence due to cross-correlated fluctuations of dipole-dipole couplings and anisotropic shifts in NMR of N-15, C-13-labeled biomolecules, *J. Am. Chem. Soc.* **121**, 6876–6883 (1999).
13. A. Kumar, R. C. R. Grace, and P. K. Madhu, Cross-correlations in NMR, *Prog. NMR Spect.* **37**, 191–319 (2000).
14. K. Pervushin, R. Riek, G. Wider, and K. Wüthrich, Attenuated T-2 relaxation by mutual cancellation of dipole-dipole coupling and chemical shift anisotropy indicates an avenue to NMR structures of very large biological macromolecules in solution, *Proc. Natl. Acad. Sci. USA* **94**, 12,366–12,371 (1997).
15. R. Riek, G. Wider, K. Pervushin, and K. Wüthrich, Polarization transfer by cross-correlated relaxation in solution NMR with very large molecules, *Proc. Natl. Acad. Sci. USA* **96**, 4918–4923 (1999).
16. G. Lipari and A. Szabo, Model-free approach to the interpretation of nuclear magnetic resonance in macromolecules, *J. Am. Chem. Soc.* **104**, 4546–4559 (1982).
17. K. Pervushin, G. Wider, R. Riek, and K. Wüthrich, The 3D NOESY- $[^1H, ^{15}N, ^1H]$ -ZQ-TROSY NMR experiment with diagonal peak suppression, *Proc. Natl. Acad. Sci. USA* **96**, 9607–9612 (1999).
18. E. Fraenkel and C. O. Pabo, Comparison of X-ray and NMR structures for the Antennapedia homeodomain–DNA complex, *Nature Struct. Biol.* **5**, 692–696 (1999).
19. A. J. Dingley, J. M. Masse, R. D. Peterson, M. Barfield, J. Feigon, and S. Grzesiek, Internucleotide scalar couplings across hydrogen bonds in Watson–Crick and Hoogsteen base pairs of a DNA triplex, *J. Am. Chem. Soc.* **121**, 6019–6027 (1999).
20. H. Benedict, I. G. Shederovich, O. L. Malina, V. G. Malkin, G. S. Denisov, N. S. Golubev, and H. Limbach, Nuclear scalar spin–spin couplings and geometries of hydrogen bonds, *J. Am. Chem. Soc.* **122**, 1979–1988 (2000).
21. K. Wüthrich, “NMR of Proteins and Nucleic Acids,” Wiley, New York (1986).
22. M. Piovto, V. Saudek, and V. Sklenar, Gradient-tailored excitation for single-quantum NMR-spectroscopy of aqueous-solutions, *J. Biomol. NMR* **2**, 661–665 (1992).
23. H. Geen and R. Freeman, Band-selective radiofrequency pulses, *J. Magn. Reson.* **93**, 93–141 (1991).
24. L. E. Kay, P. Keifer, and T. J. Saarinen, Pure absorption gradient enhanced heteronuclear single quantum correlation spectroscopy with improved sensitivity, *J. Am. Chem. Soc.* **114**, 10,663–10,665 (1992).
25. C. Fernández, T. Szyperki, A. Ono, H. Iwai, S. Tate, M. Kainosho, and K. Wüthrich, NMR with $^{13}C, ^{15}N$ -doubly-labeled DNA: The Antennapedia homeodomain complex with a 14-mer DNA duplex, *J. Biomol. NMR* **12**, 25–37 (1998).
26. A. T. Brünger, Crystallographic refinement by simulated annealing: Methods and applications, *Methods in Enzymology* **277**, 366–396 (1997).